Nat Hazards (2010) 54:75–95
DOI 10.1007/s11069-009-9454-4

ORIGINAL PAPER

Tsunami vulnerability assessment of Casablanca-Morocco using numerical modelling and GIS tools

R. Omira · M. A. Baptista · J. M. Miranda · E. Toto · C. Catita · J. Catalão

Received: 13 May 2008 / Accepted: 24 August 2009 / Published online: 24 September 2009

Abstract Earthquakes and tsunamis along Morocco's coasts have been reported since historical times. The threat posed by tsunamis must be included in coastal risk studies. This study focuses on the tsunami impact and vulnerability assessment of the Casablanca harbour and surrounding area using a combination of tsunami inundation numerical modelling, field survey data and geographic information system. The tsunami scenario used here is compatible with the 1755 Lisbon event that we considered to be the worst case tsunami scenario. Hydrodynamic modelling was performed with an adapted version of the Cornell Multigrid Coupled Tsunami Model from Cornell University. The simulation covers the eastern domain of the Azores-Gibraltar fracture zone corresponding to the largest tsunamigenic area in the North Atlantic. The proposed vulnerability model attempts to provide an insight into the tsunami vulnerability of building stock. Results in the form of a vulnerability map will be useful for decision makers and local authorities in preventing the community resiliency for tsunami hazards.

Keywords Tsunami · Vulnerability · Numerical modelling · Inundation · GIS · Casablanca

R. Omira · E. Toto
Faculty of Sciences, University Ibn Tofail, Kénitra, Morocco

M. A. Baptista
Instituto Superior de Engenharia de Lisboa, Lisbon, Portugal

R. Omira (✉) · M. A. Baptista · J. M. Miranda
Faculdade de Ciências de Lisboa, CGUL, IDL, University of Lisbon, Edifício C8, 3°, Campo Grande, 1749-016 Lisbon, Portugal
e-mail: omirarachid10@yahoo.fr

C. Catita · J. Catalão
LATEX, IDL, University of Lisbon, Lisbon, Portugal

1 Introduction

Morocco, by its peculiar geological context and proximity to the Nubia–Eurasia plate boundary (NEPB) is the western African littoral that is most exposed to earthquake-induced tsunamis (El Alami and Tinti 1991). The most severe submarine earthquakes felt in Morocco were those generated offshore along the Atlantic coast (El-Mrabet 1991). Some of these events were tsunamigenic, as was the case of the 1st November 1755 event, which certainly was the most devastating tsunami ever reported in Morocco. Its waves ravaged the Iberian and Moroccan Atlantic coasts, with run-up heights that reached 5–15 m and were observed across the Atlantic in the West Indies (Baptista et al. 1998a; Lander et al. 2002, 2003). The largest Atlantic earthquakes of the last century were the 25th November 1941 ($M = 8$) strike slip event (Buforn et al. 1988, 2004) and the 28th February 1969 ($Ms = 7.9$) event (Fukao 1973). Both events were recorded in Morocco. The peak-to-peak amplitudes of the 1941 event were 0.23 and 0.5 m (1.30 and 1.40 m with the tide) at the "Casablanca-Jetée Trasversal" and "Casablanca-Petite Darse" tide gauge stations, respectively (Debrach 1946). In the case of the February 1969 event, the unique record available to us is a hand copy drawing of the filtered signal showing a first arrival of 0.9 m downward.

The present study reviews the impact of tsunami inundation on the Atlantic coast of Morocco by assessment of the associated vulnerability. The extensive occupation of the coastal area, the enormous influx of tourists during high season and the great importance of harbours and other coastal facilities increase considerably the vulnerability of the Atlantic coastal regions of Morocco to tsunami impact. However, tsunami-related vulnerability studies have never been attempted along the Moroccan coast, which makes this study a first-hand quantification of the tsunami hazard in the region. Mapping vulnerability is required for preventing the community resiliency and emergency planning for tsunami hazards, especially in the areas where the tsunami threat is poorly estimated.

The area studied of about 10 km × 2 km, corresponds to Casablanca harbour and its surroundings (Fig. 1a). This part of Casablanca includes several historical and cultural sites, such as the Sqala, and more generally the ancient Medina, the modern Hassan II Mosque, and a wide range of building types with a variety of styles (traditional Arab, colonial French, and more modern buildings). It is characterized by a population of about 550,000 inhabitants who are concentrated in the main districts of Sidi Belyout, Roches Noires, ancient Medina and El Hank. Moreover, the area has very great economic importance due to the presence of the harbour, which is the most important in Morocco. Hence, in case of a tsunami inundation, the economic and human loss in the study area could be considerable. Also, the flat topography of the region (Fig. 1b) increases the risk of inundation in this part of Casablanca.

In this study, we compute the tsunami inundation boundary, the inundation flow depth and the vulnerability of building stock in the area. The paper is subdivided into two sections. The first focuses on tsunami hydrodynamic modelling and inundation mapping, whereas the second concerns the development of a new tsunami vulnerability calculation model, which can be used to assess the building vulnerability of large areas with a variety of building structures. The tsunami vulnerability assessment approach presented here is based on a combination of the results of tsunami hydrodynamic modelling, information collected during the building inventory and the use of a GIS tool to construct vulnerability maps. A step-by-step methodology that considers three parameters/criteria to be the main elements that influence the tsunami vulnerability of buildings was developed. These

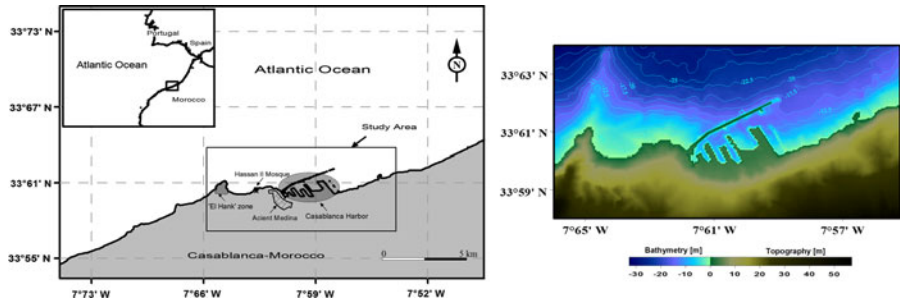

Fig. 1 **a** The study area of Casablanca-Morocco. **b** Bathymetry and topography for the Casablanca Harbour and its surrounding areas

parameters/criteria are building condition, inundation zone and quality of sea defence. A dynamic calculation formula, which uses the three criteria, is developed and presented.

2 Geological background—tectonic tsunami models

The study sector is centred on the Casablanca harbour and represents an area of about (10 × 2) km^2 (Fig. 1a). This segment of the North Atlantic coast of Morocco is located at the western end of the Nubia–Eurasia plate boundary (NEPB). The NEPB extends from the Azores to the western Mediterranean Sea, showing contrasting tectonic features from transtensional in the west, close to the Azores, to transpressional at the Gibraltar Strait (Buforn et al. 1988; Morel and Meghraoui 1996; Roest and Srivastava 1991; Jiménez-Munt et al. 2001) (Fig. 2). Along the Azores, the interplate domain is rather complex, as a consequence of the low spreading velocity (ca. 5 mm/year), but it generates spreading along the Terceira and Pico–Faial axes (Miranda et al. 1998; Fernandes et al. 2007). Between 24°W and 19°W, it is believed to follow a prominent morphological feature, the Gloria Fault, in an almost pure transcurrent way. East of 19°W, the interplate domain is morphologically complex and characterized by a series of huge ridges and seamounts (the Gorringe Bank, the Coral Patch and Ampère seamounts) that delimitate morphological depressions, such as the Horseshoe and Tagus abyssal plains, where discrete segments of plate boundary are difficult to identify (Sartori et al. 1994; Tortella et al. 1997). East of 19 W, the focal mechanisms indicate right lateral and reverse faulting on roughly east–west oriented structures (Borges et al. 2001; Buforn et al. 2004). This is usually interpreted as being the result of the relatively low interplate motion (ca. 4 mm/year) given by kinematic plate models (e.g., DeMets et al. 1994; Sella et al. 2002; Fernandes et al. 2003).

Almost all major earthquake events in SW Iberia are historical (pre-instrumental), although some relevant shocks have been recorded by instruments during the last century. Among the historical events, the 1st November 1755 event is the best described. However, as a consequence of the complexity of this transpressive domain, the location of the earthquake source remains uncertain. The descriptions of the previous large events may be obtained only from a few Roman documents that we cannot access at this stage. Also, we do not know whether they correspond to different events on broadly the same geological structure or to the activity of different segments of the plate boundary.

On the other hand, several authors have investigated the source of the Lisbon earthquake, using either macroseismic data (Martinez-Solares et al. 1979; Levret 1991), average

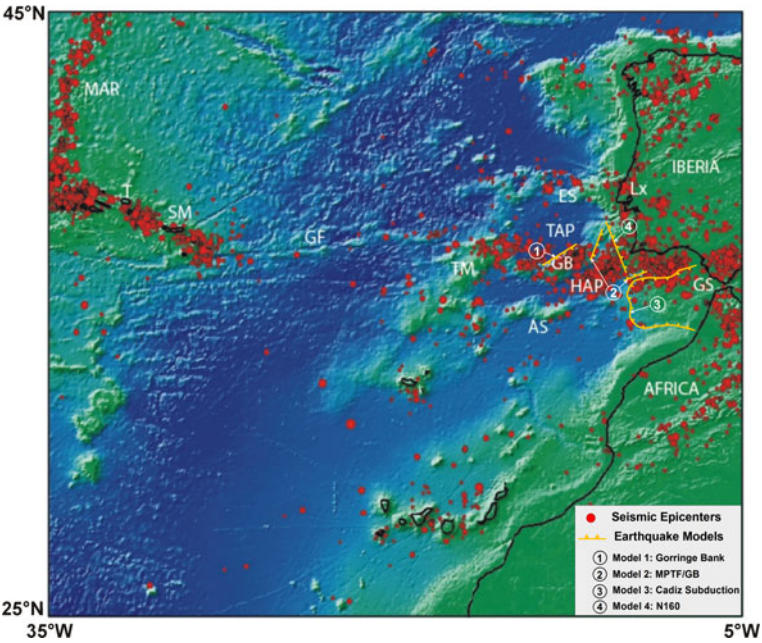

Fig. 2 Seismicity map of the Azores-Gibraltar area and the 1st November 1755 Lisbon model earthquakes used in this study. Seismic Data (*red dots*) from ISC Catalogue for the period 1970–2007 and magnitudes larger than 3. *T*, Terceira Island; *HAP*, Horseshoe Abyssal Plain; *TAP*, Tagus Abyssal Plain; *GF*, Gloria Fault; *SM*, S. Miguel Island; *MAR*, Mid-Atlantic Ridge; *AS*, Ampère Seamount; *GB*, Gorringe Bank; *ES*, Estremadura Spur; *GS*, Gibraltar Straight. Earthquake models (*yellow traces*): (*1*) Gorringe Bank North (Johnston 1996), (*2*) Pop up model (Zitellini et al. 1999; Baptista et al. 2003), (*3*) Cadiz Slab (Gutscher et al. 2002) and (*4*) N160 (Baptista et al. 1998b)

tsunami amplitudes in the tide records of the 28th February 1969 tsunami (Abe 1979), or scale comparisons with the 1969 event (Johnston 1996). These studies were based on the assumption that the 1755 earthquake source was located south of the Gorringe Bank in the Horseshoe Abyssal Plain close to the 1969 earthquake and tsunami source (Gjevik et al. 1997), and most probably related to the bank build up (Fukao 1973). A different approach was considered by Baptista et al. (1998a, b) in a systematic study of the historical records of the 1755 tsunami wave heights observed along the Iberian and Morocco coasts. It was based on tsunami hydrodynamic modelling that was concluded for a different source position that was located closer to the SW Portuguese continental margin. The approach taken by Baptista et al. (1998b) was not to deduce "the source" from tsunami data, but to deduce the constraint on the location of the source by tsunami data. Independently, Zitellini et al. (1999), based on the outcome of a regional MCS survey performed in 1992 (AR92 lines), identified a very large active, compressive, tectonic structure located 100 km off-shore SW Cape S. Vicente, which was proposed as a likely cause of the 1775 event. This location was compatible with the numerical modelling of Baptista et al. (1998a, b). Finally, an alternative solution was proposed by Gutscher et al. (2002) based upon seismic images of the crustal structure in the Gulf of Cadiz and tomographic images that indicate an active accretionary wedge, overlying an eastward dipping basement and connected to a steep, east dipping slab of cold, oceanic lithosphere beneath Gibraltar. Gutscher et al. (2002) used the geometry of the shallow east dipping fault plane of the Gibraltar subduction as determined

Table 1 Fault parameters for different earthquake models for the 1st November 1755 Lisbon tsunami

	Source name	Fault parameters				
		Dimension (km)	Slip (m)	Dip (°)	Strike (°)	Rake (°)
Model 1	Gorringe Bank source (Johnston 1996)	$L = 200$; $W = 80$	12	40	56.7	90
Model 2	MPTF/GB source (Zitellini et al. 1999)–(Baptista et al. 2003)	MPTF: $L = 105$; $W = 55$ GB: $L = 96$; $W = 55$	20	24	21.7 258.5	90
Model 3	Cadiz subduction source (Gutscher et al. 2002; Gutscher 2004)	$L = 210$; $W = 180$	10	2.5; 5 and 7.5	349	90
Model 4	N160 source (Baptista et al. 1998b)	$L = 210$; $W = 75$	13	45	340	90

in a parallel study (Thiebot and Gutscher 2006) and calculated the ensuing seismic moment. He also modelled synthetic tsunami waves generated by rupture along such a fault plane.

For this study, we selected four different earthquake models, which are thought had generated the 1st November 1755 earthquake (Fig. 2). Considering that the latter corresponds to the worst case earthquake scenario, we assume that these earthquake models represent the WYCC (Worst Yet Credible Case) of a tsunami impacting Casablanca. All earthquake models infer a magnitude of $\sim$8.3–8.5. The fault parameters presented in Table 1 correspond to those published by Johnston (1996), Zitellini et al. (1999, 2001), Baptista et al. (1998b, 2003), Gutscher et al. (2002, 2006), Gutscher (2004), and are used to compute the sea bottom deformation in the Okada's equations (Mansinha and Smylie 1971; Okada 1985). A comparison of different earthquake mechanisms is beyond the scope of this study.

3 Mapping inundation

3.1 Numerical model

The tsunami hydrodynamic modelling includes three main steps—generation, propagation and inundation (Liu et al. 1994). To generate the initial disturbance of the ocean surface by a submarine earthquake, the initial sea surface perturbation is assumed to be equal to the vertical displacement of the sea floor. The deformation of the ocean bottom is determined from a linear elastic dislocation theory (Mansinha and Smylie 1971; Okada 1985). Tsunami propagation and run-up calculations were based on a modified version of the Cornell Multigrid Coupled Tsunami Model (COMCOT) (Liu et al. 1998), which we have named COMCOT-Lx. The code solves both linear and non-linear shallow water equations in spherical or Cartesian coordinates using an explicit leap-frog finite difference numerical scheme (Liu et al. 1998). The numerical model uses a nested grid system with different grid resolutions in order to fulfil the need for tsunami simulations in different scales—from the source zone to the high resolution local grids where inundation maps are computed (Wang and Liu 2007b).

A moving boundary scheme (Liu et al. 1995) to track the moving shoreline enables the run-up and the inundation to be computed. The effect of bottom friction on tsunami flooding is taken into account by Manning's formula. The reliability of COMCOT-Lx was tested against the benchmark tests proposed by Synolakis et al. (2007). The COMCOT code has been used to study several tsunami events such as the 2003 Algeria Tsunami (Wang and Liu 2005) and, more recently, the 2004 Indian Ocean tsunami (Wang and Liu 2007a).

3.2 Digital terrain model (DTM)

The grid model for simulation of tsunami propagation in the eastern part of the Atlantic Ocean offshore from Morocco and the Gulf of Cadiz extends from 30°N to 42°N and from 4°W to 13°W. To obtain a good description of bathymetric and topographical effects, three nested grid layers of differing resolutions (0.008°, 0.002° and 0.0005°, corresponding to 800, 200 and 50 m) were incorporated. The finer or high resolution grid is focused on Casablanca harbour and its surroundings (Fig. 1b). The DTM (bathymetry/topography) was generated from a compilation of multisource height/depth data from multibeam surveys, digitalized bathymetric charts of 1:150,000 and 1:15,000 scales (Folio 3,132 and 861 of Admiralty Charts and publications) and digital cartographic data of 1:25,000 scale. Small and large scale bathymetric charts were merged on a unique database, and all data was transformed to WGS84/UTM coordinates (fuse 29). For the shore, digital height data from 1:25,000 topographical charts were supplied by "Direction de la Conservation Foncière du Cadastre et de la Cartographie" of Morocco.

The fusion of high resolution depth and height data requires a common definition for the vertical reference surface. Bathymetric charts and topographical charts use different vertical references. The first uses a local reference related to the principal harbour of the chart and the later uses the mean sea level for a certain epoch. In this project, the zero height (vertical datum) was defined by the General levelling network of Morocco as the mean sea level for the Casablanca tide gauge, and all depths were converted to this reference.

The zero height contour line that was obtained from the 1:25,000 topographical data was then used as a boundary for land–sea transition. Depth and height data were merged subjected to the zero line constraint and carefully edited on the onshore–offshore envelope. A TIN (triangular irregular network) with all data points, including the zero height line as a constraint and breaklines representing surface discontinuities close to the shoreline (harbour, pier, quay), was constructed. A second editing was done and a final grid with 10 m resolution was computed over the TIN network. Generalizing the 10-m resolution grid to a 50-m resolution grid, which is necessary for the modified COMCOT program, has an enormous smoothing effect that destroys most of man-made structures. In order to preserve these main structures, an enhancement/exaggeration scheme was applied to the 10-m resolution grid before the generalization to a 50-m grid. In the DTM, there is no inclusion of breakwater structures or buildings. The estimated vertical accuracy on land is 2 m, estimated as the standard deviation of the residuals between the grid (50 m resolution) and the cartographic data. This varies significantly, mainly in the sea, according to the existing charts.

3.3 Mapping inundation results

Figure 3 shows the results of inundation computations and flow depths over land for each proposed earthquake model. These results do not take into account the tide. As expected,

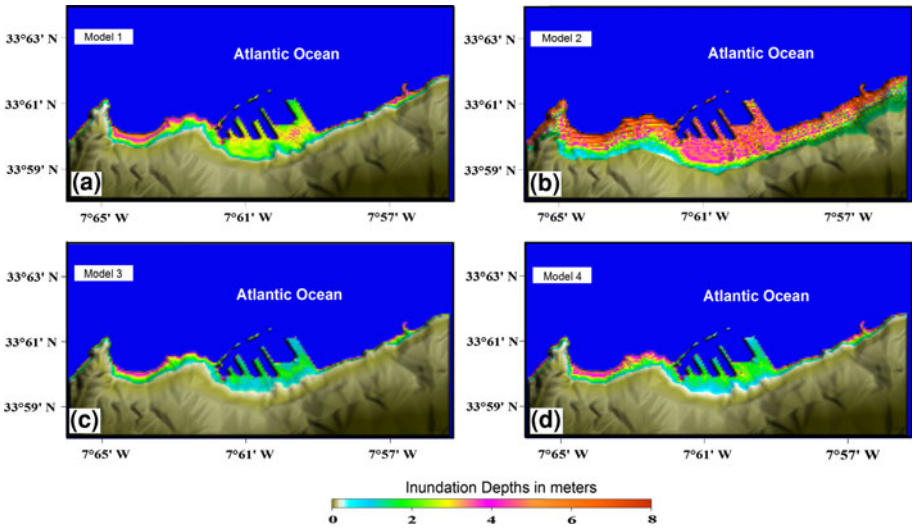

Fig. 3 Inundated area and computed flow depths over land for each proposed source model of the 1st November 1755 Lisbon earthquake and tsunami

the presence of flat low areas close to the sea (Fig. 1b) makes this site prone to tsunami flooding. All rupture mechanisms that were tested produced an inundation of the Casablanca harbour and surrounding area to a distance of approximately 1.5 km inland. Tsunami flow depths vary from 1 to 6 m at Casablanca harbour and its surroundings. In all cases, the maximum run-up is compatible with the slip value of the rupture mechanism, as already noted by Okal and Synolakis (2004). A maximum flow depth of $\sim$6 m is obtained for candidate earthquake model 2. Flow results from this model represent the most extreme inundation case for the study area. In the case of the three other models, the inundation is less than in the previous case.

4 Building tsunami vulnerability (BTV) assessment

4.1 Building survey

The area that today is Casablanca was settled in about the tenth century BC. It was since used as a port by the Phoenicians and, later, the Romans. During the fourteenth century, the town rose in importance as a port. In the fifteenth century, it was destroyed by the Portuguese, who used the ruins to build a military fortress in 1515. The village that grew up around it was called, according to some sources, "Casabranca", meaning "White House" in Portuguese. The Portuguese eventually abandoned the area completely after 1755, following the earthquake that destroyed it. The Old Town and the ancient Medina, as it is today, was built during the eighteenth century and continued to develop during the Spanish period. During the French occupation (1907–1956), some French style buildings appeared next to the Old Town. The development of the industrial harbour of Casablanca began under the French occupation, but the work was completed only in 1912.

The authors visited the coastal area of Casablanca in April 2007, to perform an inventory of the building types and the quality of existing sea defences. The survey concentrated on the harbour and surrounding areas (Medina, Ain Sebaa) and attempted to examine the condition of buildings, as well as their possible capacity to resist tsunami waves.

The area is characterized by the presence of a large variety of structure types ranging from non-engineered buildings to well-designed engineered constructions. The non-engineered structures include single-storey unreinforced brick houses and low-rise timber buildings, stores typical of the ancient Medina and two- or three-storey reinforced concrete frame structures. On the other hand, multi-storey engineered structures are in the form of reinforced concrete (RC)-framed buildings with masonry infill or concrete block walls. Six types of constructions were distinguished (Fig. 4a–f): unreinforced masonry walls, timber construction, brick traditional, non-engineered RC buildings, engineered RC frames with infill masonry walls and multi-storey engineered RC buildings. The main features and detailed descriptions of these building types are as follows:

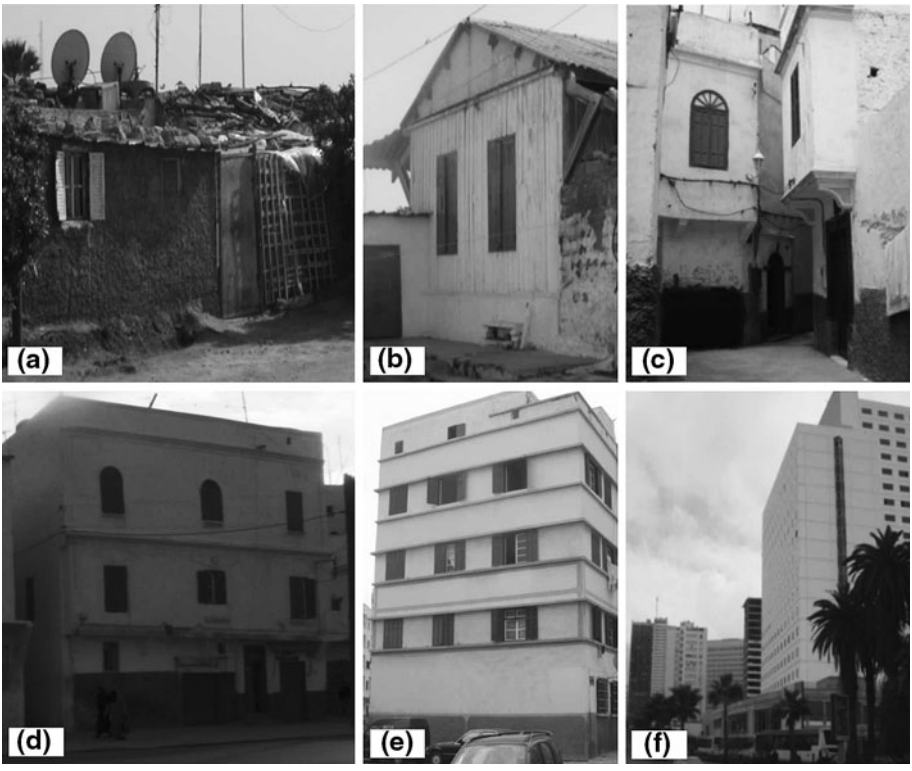

Fig. 4 Building types in the study area. **a** Single-storey structureless dwelling; **b** non-engineered timber construction; **c** brick traditional buildings of the ancient Medina; **d** non-engineered RC building with masonry infill walls; **e** engineered RC frames with infill masonry walls; **f** multi-storeys well-designed engineered RC buildings

4.1.1 Unreinforced masonry walls

The single-storey structureless dwellings of 2.5–3 m in height are the predominant type in the 'El Hank' coastal zone of Casablanca. The construction of this building type consists of masonry bricks or dry stones with earthen mortar walls, without reinforced concrete columns or beams. They are also characterized by very shallow foundations. Most roofs are zinc coated and few are covered by wood and cement mortar.

4.1.2 Timber construction

Non-engineered timber constructions were observed in the western coastal part of the studied area, about 5 km from the harbour ('El Hank' zone). Single-storey residential buildings of this category are among the minority in this sector. These houses have timber plank walls, wood frames and beams that are attached to typical galvanized iron sheet roofs. Most houses suffer from very shallow bases where the columns are not well anchored to the foundation.

4.1.3 Brick traditional

In the area next to the harbour, the typical two- or three-storey buildings of the ancient Medina form the predominant structural type for houses, shops and tourist flats. Houses are generally built by an assemblage of traditional and natural materials, such as stone, wood, lime and mortar. Buildings have rubble stones with lime mortar walls, wooden columns and beams. Roofs consist of wooden frames and layers of reeds covered with clay mortar.

4.1.4 Non-engineered RC buildings

Reinforced concrete structures in the form of two- or three-storey residential houses, cafes and shops have cracks of varying degree in their structural and non-structural elements, because of the poor quality of materials used. Such construction consists of thin columns and beams of reinforced concrete with infill unreinforced masonry bricks walls and solid slabs, with concrete roofs. At several buildings, failures of beams at joints were observed. These are related to inadequate anchorage of the reinforcing bars.

4.1.5 Engineered RC frames with infill masonry walls

This type of construction constitutes the predominant structural type in the study area. Most of these buildings are residential houses, although a few constitute the harbour facilities. Such buildings consist of reinforced concrete columns and beams of medium thickness, with infill of masonry bricks walls and solid slabs with concrete roofs. Foundations are relatively well built using stony blocks, reinforced with concrete.

4.1.6 Multi-storey engineered RC buildings

These well-designed buildings are the predominant type of structure for hotels, offices and also new residential apartments. These twentieth-century multi-storey constructions were built in accordance with the Moroccan paraseismic code (RPS 2000). This category of buildings is characterised by robust reinforced concrete columns and beams connected to

concrete block bearing walls and/or masonry infill walls. The roofs consist of precast concrete beams with concrete topping.

In summary, poorly constructed structures in the form of low-rise timber houses, unreinforced masonry walls or non-engineered RC buildings appear to be the most vulnerable to tsunami forces and can suffer varying degrees of damage, depending on their location from the shore. However, the well-designed engineered structures appear to possess sufficient strength to resist tsunami lateral forces, which can survive tsunami waves with minor damages that will be limited to the first floor.

4.2 BTV assessment methodology

In recent studies of tsunami vulnerability assessment, the dynamic concept implies that vulnerability is not uniformly distributed within the flood zone and depends on a number of parameters (Papathoma and Dominey-Howes 2003; Papathoma et al. 2003; Dominey-Howes and Papathoma 2007).

In the present study, we attempt to predict the building tsunami vulnerability of the Casablanca area using a combination of the tsunami inundation results and the information collected during the survey. A dynamic database is constructed in order to include the results of the building and sea defence survey. This database can be updated whenever needed and new vulnerability maps can be produced. GIS tools are used to display vulnerability maps. The outline of the main steps for the assessment of BTV follows:

4.2.1 Step 1: Identification and calibration of criteria controlling the BTV

The key to the BTV assessment methodology presented here is the identification of the factors that control the expected building damage related to the impact of tsunami waves. Three parameters/criteria are considered to influence the vulnerability of the building stock. They are the building condition, the inundation zone and the quality of the sea defence. The first criterion is linked to the building state, whereas the two others are related to its location. The choice of reported parameters is based on recent published studies about the performance of structures after the tragic event of Sumatra 2004. Following that event, it was observed that the level of building damage correlated well with condition of the house, construction technique, building location and water depth (Boen and EERI 2006; Maheshwari et al. 2006; Murty et al. 2006; Ruangrassamee et al. 2006; Saatcioglu et al. 2006).

However, these parameters do not affect the BTV equally. Thus, weight factors (F_w) are introduced to calibrate those elements in the order of their importance to influence building vulnerability. The importance of the criteria is considered to be linked to the measures of tsunami impact reduction that may be taken. It is easier and cheaper to improve housing conditions by reinforcement or restoration than to relocate the building or to construct a breakwater. Moreover, the reinforcement of buildings may serve to protect houses from other natural disasters. Hence, we assume that the criterion concerning the condition of buildings is higher in importance than those related to their location (inundation zone and the presence or absence of breakwaters). On the other hand, the presence of a sea defence at various places along the coastline can reduce the flood risk, but certainly not prevent a tsunami inundation, especially in the case of a great tsunami like the 1755 event. This is why the flow depth parameter is considered to be more important than the sea defence criterion in the BTV estimation model. Weighting factors (F_w) for the identified parameters/criteria are given in Table 2.

Table 2 Parameters/criteria responsible to control the BTV and corresponding weight factors (F_w)

Parameters/criteria	Weigh factor ($F_{w.i}$)
Building condition	$F_{w.b} = 3$
Inundation zone	$F_{w.i} = 2$
Sea defence	$F_{w.s} = 1$

4.2.2 Step 2: Classification connected to each criterion

In view of the fact that each identified criterion regroups a number of elements that are characterized by different levels of building performance, flood risk or resistance to tsunami wave, a classification connected to the parameters/criteria is required in order to group elements with similar conditions in a set of classes. A level of condition, risk or resistance is attributed to each established class in order to indicate its degree of vulnerability within the corresponding criterion (independently of the other criteria).

Classification of built stock is based on building inventory information. House classes are established according to building structures, material used, condition of ground soil and construction quality. Inundation maps from modelling results are used firstly to identify the flood zone and secondly to divide this zone into subzone classes, according to the computed maximum flow depths. The sea defence classes are classified according to their possible capacity to reduce tsunami inundation, taking into account their quality, form and dimensions.

A classification factor (F_c) is attributed to each established class in order to indicate its vulnerability level in relation to the corresponding criterion. The values attributed to the classification factors depend on the study area. The classification factors for the Casablanca case are discussed in Sect. 4.3.

4.2.3 Step 3: BTV estimation model

The estimation of BTV requires a combination of the criteria responsible for controlling tsunami building damage. In this study, we consider the influence of the three defined criteria in assessing the BTV for each building class. The dynamic aspect of vulnerability is taken into account by introducing the weighting and classification factors in a dynamic formula. The following formula has been adopted to assess the BTV for each building class (Eq. 1):

$$\mathrm{BTV}(\%) = \frac{(F_{c.b} \times F_{w.b}) + (F_{c.i} \times F_{w.i}) + (F_{c.s} \times F_{w.s})}{\sum_{k=1}^{3} (F_{c.\max} \times F_w)_k} \times 100 \qquad (1)$$

where $F_{c.b}$ is the building classification factor corresponding to the building class for which the BTV is calculated; $F_{c.i}$ corresponds to the classification factor of the flood zone class where the building class is located; and $F_{c.s}$ is the classification factor of the sea defence class existing in front of the building class. $F_{w.b}$, $F_{w.i}$ and $F_{w.s}$ are the weighting factors for building condition, inundation zone and sea defence, respectively. $F_{c.\max}$ is the maximal value of the classification factor established in the k-criterion; where k is the criterion number.

On the other hand, the values of the BTV calculated from the Eq. 1 are associated with a grade of expected building damages. Five categories of building damage levels, ranging from *D0* (no damage) to *D4* (total destruction), are considered. Each grade of damage is

defined to describe an interval of the estimated building vulnerability in order to give a clear idea of what concern the limits of mechanical resistance of buildings against the tsunami flood. The *D0* grade corresponds to a BTV of 0–20%; *D1* (slight no structural damage) to a BTV of 20–40%; *D2* (slight structural damage) to a BTV of 40–60%; *D3* (severe structural damage) to a BTV of 60–80% and, finally, *D4* (total collapse) to a BTV of 80–100%.

4.3 Application to the study area

4.3.1 Building classification

Engineered and non-engineered buildings in the study area (Sect. 4.1) were classified into four main categories—class A to class D (Table 3). In order to describe each building class, levels of structure condition and performance are attributed, and a corresponding classification factor ($F_{c.b}$) is established. The main characteristics of building construction, such as its quality, the material used and the number of storeys were taken into account to estimate the building performance level. Five levels, ranging from very good for well-designed buildings to bad for structureless dwellings, are attributed. The $F_{c.b}$ is defined according to the level of performance that each building class can develop in the case of a tsunami threat, considering only the building condition criterion. For this reason, building class A, including single-storey structureless dwellings and timber buildings, is considered to be four times greater in order of vulnerability than building class D, which consists of well-designed multi-storey engineered buildings.

Table 3 Building classification, structure conditions, mechanical resistance and classification factors ($F_{c.b}$) of building stock along the study area

Building class	Structure, material used, construction quality	Condition level	Mechanical resistance and expected damage	Classification factor ($F_{c.b}$)
A	Single-storey structureless dwelling and timber buildings made of unreinforced bricks, stone, earthen mortar, wood and zinc. Very poor construction quality	Bad	Very weak resistance to lateral forces: risk of total collapse in case of a great tsunami	4
B	Traditional brick houses of the ancient medina made of stone, wood, lime, reed and clay mortar. Non-engineered two- or three-storeys RC with unreinforced masonry walls and thin RC frames. Medium construction quality	Medium	Weak resistance to lateral loads, acceptable resistance to the horizontal forces. Risk of severe structural damage in case of a great tsunami	3
C	Two to four-storeys engineered RC-framed buildings with infill masonry walls. Good construction quality	Good	Good resistance to both lateral and horizontal forces. Risk of slight to moderate damage	2
D	Well-designed multi-storeys engineered new buildings with robust RC frames and concrete block walls. Very good construction quality	Very good	Strong resistance to both lateral and horizontal forces. Only slight damage is expected	1

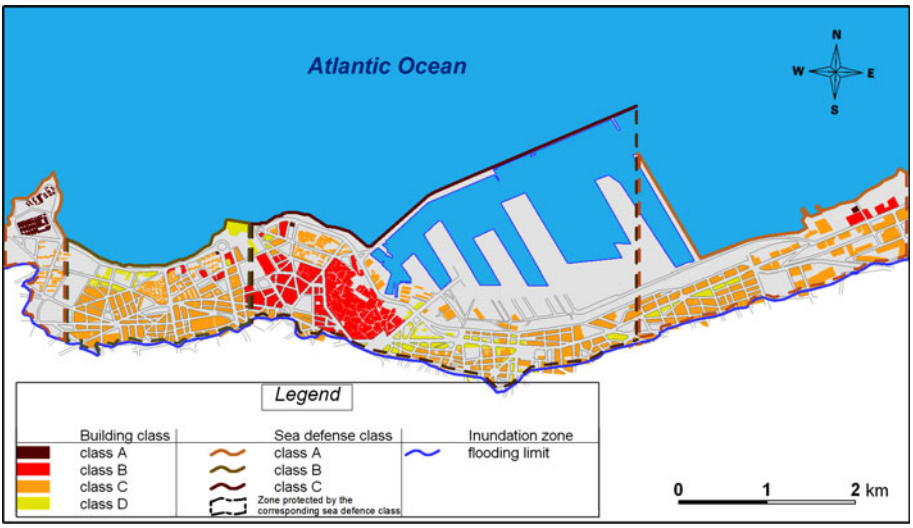

Fig. 5 Map to display the distribution of the established building and sea defence classes within the inundation zone

A summary of the building classification and present structural conditions is given in Table 3. The distribution of the different building classes within the inundation zone is illustrated in Fig. 5.

4.3.2 Identification and classification of zones prone to tsunami inundation

The identification of zones of potential inundation is based on the results of tsunami inundation modelling that are presented in Sect. 3. For tsunami vulnerability assessment, we take the most extreme result (model 2) from the various models studied as a case to study. The classification of flooded subzones at significant risk shows that we can divide the inundation zone into three levels based upon the flow depths obtained from the inundation maps. Table 4 presents the inundation risk level, the corresponding flow depth and the classification factor ($F_{c.i}$) for each classified inundation subzone. The $F_{c.i}$ varies from 3 for 4–6 m of flow depth to 1 for 0–2 m of inundation, depending on the flooding risk level. The $F_{c.i}$ values are based on the assumption that the 1755 event represents the worst case tsunami for the study area. The flow depths of 4–6 m are considered to be the maximum that can be produced in this area. This is why the higher class value of 3 is attributed to 4–6 m of inundation.

Table 4 Inundation subzones classes; the corresponding inundation risk levels, flow depths and classification factors ($F_{c.i}$)

Zone class	Inundation risk level	Corresponding flow depth (m)	Classification factor ($F_{c.i}$)
A	High	4–6	3
B	Medium	2–4	2
C	Low	0–2	1

Table 5 Sea defence classes; the corresponding characteristics, resistance levels and classification factors ($F_{c.s}$)

Sea defence class	Characteristics	Resistance level	Classification factor ($F_{c.s}$)
A	Absence of sea defence	Bad	3
B	Concrete wall of about 5 m in height and 0.6 m in thickness	Medium	2
C	Tetrapods of 3 m in height + 3-m high concrete walls	Good	1

4.3.3 Classification of sea defence quality

The field survey revealed areas that are relatively well protected from moderate tsunami waves and also areas where there is almost no sea defence. The existing sea defence structures consist of: (1) tetrapod concrete breakwaters of about 3 m in height each, which are superposed and distributed around the harbour and the Hassan II Mosque, (2) a concrete revetment wall of about 5 m in height and 0.6 m in thickness, which extends ~2.5 km along the coastline between the Hassan II Mosque and the El Hank zone and (3) 3-m high concrete walls constructed onshore, a few meters from the shoreline and covering the area from the harbour to the Hassan II Mosque.

In Table 5, we classify the various existing sea defence structures, according to their possible capacity to resist tsunami waves. The good level of resistance is attributed to the breakwater structures, including both tetrapods and the 3-m high concrete walls, which protect the harbour zone up to the Hassan II Mosque (Fig. 5). A medium level is considered for the revetment breakwater in the form of the 5-m concrete wall (Fig. 5). However, the areas, where sea defence structures are absent, appear to offer poor levels of resistance. A classification factor ($F_{c.s}$) is assigned to each sea defence class to indicate the breakwater class performance (Table 5).

4.3.4 Elaboration of BTV map using GIS tool

The coastal Casablanca base map that depicts an area up to 2 km from the coast was digitized from a 1:5,000 scale map using GIS software. This map is used to extract three different layers of our GIS database: building blocks, sea defence areas and inundation zones. Buildings were grouped as polygons (Fig. 5). Areas that either had or lacked sea defence structures were digitized as polygon features. Each polygon feature starts from the coastline, where the breakwater is constructed, and proceeds inland including the zone protected by the sea defence structure (Fig. 5). Inundation subzones were identified from modelling results and then digitized in our map.

Each layer was scored according to Table 2. The numerical value assigned to each unique attribute quantifies the risk associated with each attribute. Spatial Intersection functionality in ArcGIS software was used to combine all layers into a composite data set to ease the analysis. This functionality uses the logical operator "AND" to combine all of the information in "Input" with all of the information in "Overlay". The resultant "Output" contains all of the data from all layers. Once all layers were joined into a single layer, the building tsunami vulnerability was estimated by application of Eq. 1 to yield a BTV map.

4.4 BTV results and model validation

We tested the proposed BTV assessment approach in a part of the coastal area of Casablanca-Morocco that is characterized by a high building density and a large variety of construction types. Figure 6 shows the tsunami vulnerability variations for the building classes in the inundation zone and the sea defence classes. It also indicates the expected building damage in order to estimate the mechanical limits of buildings' resistance against tsunami waves. This graph was established by applying Eq. 1 to the different building classes of the study area. The results indicate that the tsunami vulnerability of each building class is significantly influenced by the criteria of building location. The BTV for class A ranges from ~72 to 100%. This makes this building category highly vulnerable to a tsunami flood with total collapse as the expected damage. The high BTV also includes buildings from class B. Their vulnerabilities vary between 57 and 85%, which correspond to a medium to high BTV. The class C building category appears to be less vulnerable than the previous categories. It has a maximum BTV of ~70%. Among the building classes of the study area, class D appears to possess good resistance to tsunami inundation, seeing that its vulnerability reaches ~55% in the worst case (class A for both inundation zone and sea defence).

The spatial distribution of the BTV in the study area is displayed in Fig. 7. The results clearly show that most buildings located near the shore within the high flood risk zone (4–6 m of flow depth) belong to the very high or high BTV category (Fig. 7). The exceptions, with a medium BTV, correspond to the well-designed structures (i.e., Hassan II Mosque and twentieth-century multi-storey buildings). The zone of medium flood risk (2–4 m of flow depth) is characterized by the presence of four levels of BTV. Within this

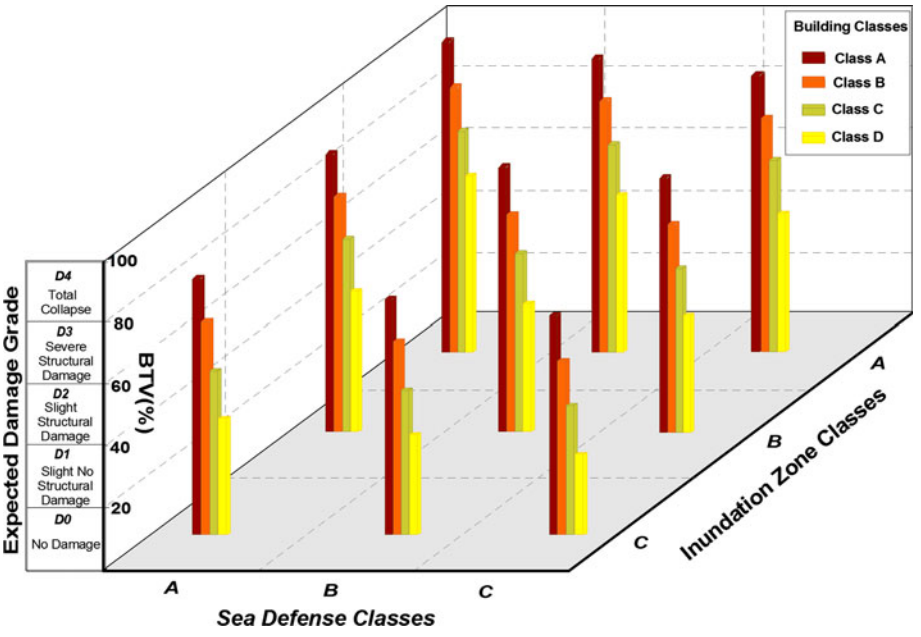

Fig. 6 Tsunami vulnerability variations for the building classes in function of the inundation zone and sea defence classes and the corresponding expected damages

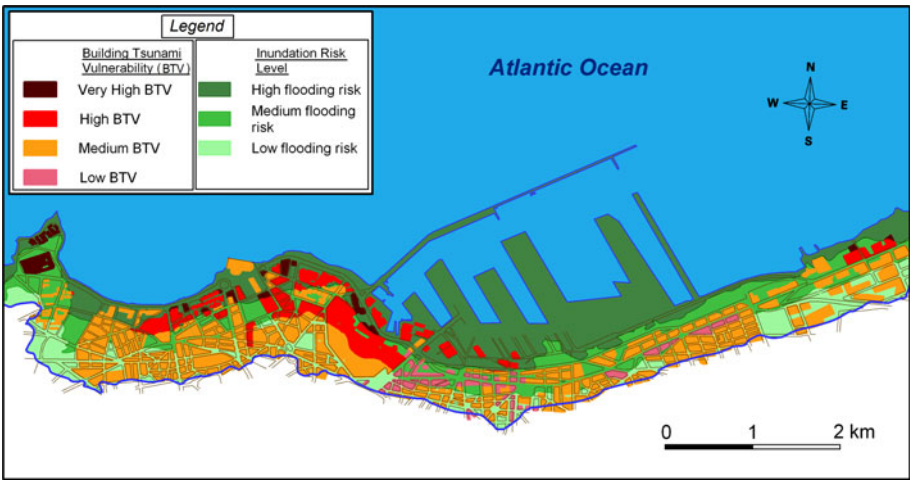

Fig. 7 Map to display the BTV within the flood zone in the study area of Casablanca-Morocco

subzone, the structureless dwellings and timber buildings, especially those located in the 'El Hank' zone, are very high vulnerable to 2–4 m of flow depth. This zone also includes ~50% of the ancient Medina structures, for which the level of vulnerability is high (60–80%). The low BTV category subsists in this flooded subzone due to the good quality of building construction and the presence of a good sea defence. The predominant category in the low flood risk zone (0–2 m of flow depth) is the medium BTV.

Like all models, the BTV model proposed in this study requires validation. For this purpose, we use the results of the field survey performed after the 17th July 2006 Java tsunami (Reese et al. 2007). This post-tsunami survey focused on Pangandaran–Indonesia, due to the high proportion of permanent buildings with much variation in design, and also the high levels of reported building damage in this area. Following Reese et al. (2007), the observed building destruction levels range from extensive damages for non-engineered structures to limited damages for well-designed engineered structures. The results of this study that involve the building categories and the corresponding observed damage levels are summarized in Table 6.

In spite of the relative differences in building structures between the study area of Casablanca and the Pangandaran area, a good correlation in term of observed damage levels (for Pangandaran) and estimated BTVs (for Casablanca) can be found. The poor structure types, involving the timber/bamboo houses, were subject to total destructions at a water depth that exceeded 2 m in Pangandaran. The observed damage is in good agreement with the estimated BTV of 80–100% for the poorly constructed buildings in Casablanca with an inundation depth of more than 2 m. Moreover, for building classes B and C of the study area, the expected vulnerability levels for a flood depth reaching 4 m correspond approximately to the damage levels observed for brick traditional and RC frame with infill walls structures in Pangandaran (Table 6). However, this validation has some limitations, especially in regard to the estimation of BTV for building class D in Casablanca and also within the inundation zone where the flood depth exceeded 4 m. These limitations are due to the fact that: (1) the Pangandaran area does not contain well-designed multi-storey buildings that are similar to those of class D in Casablanca; and (2) the water depth in Pangandaran area did not exceed 4 m.

Table 6 Observed levels of tsunami damage for the building stock in Pangandaran area after the 17th July 2006 Java tsunami

Building category	Observed damage
Timber/bamboo	For a 1.5–2 m of water depth 70% destroyed and 30% lightly to heavy damaged. For a depth exceeding 2 m, essentially a total collapse
Brick traditional	Damage levels not much deferent from timber/bamboo buildings, exception for water depth greeter than 2 m where some houses remained upright but not repairable
Brick traditional with RC columns	<1 m of water—minor damage 1–2 m of water—light to moderate damage (repairable) 3–4 m of water—serious damage, but buildings upright
RC frame with brick infill walls	<1 m of water—light damage to ground floor 1–2 m of water—light to moderate damage to ground floor (repairable) 3–4 m of water—moderate damage to ground floor (holes punched through 1 or more walls), but building upright and repairable

5 Discussions

5.1 Mapping inundation

The great inundation distances and flow depths obtained for the four candidate tsunamigenic sources suggest that coastal Casablanca communities are seriously exposed to the risk of tsunamis. The computed maximum flow depth ranges from 1 to 6 m. Several factors, such as the earthquake source parameters, earthquake location, near-shore bathymetry and coastal topography, control the variation in flow depth in the Casablanca sector. Clearly, the threat posed by a rupture mechanism of a 20-m slip (model 2) is greater than those posed by just the 10–13 m of slip (models 1, 3 and 4). The use of a 20-m slip for tsunamigenic model 2 may overestimate the computed flow depth in the study area. We also assume that the inundation results are overestimated due to the fact that the coastal sea defence structures around Casablanca harbour were not included in the DTM model. Normally, a comparison of modelling results with historical records enables one to test the reliability of the numerical results. However, the lack of precise historical reports concerning the impact of the 1755 tsunami event on the Casablanca area makes any comparison difficult. Moreover, changes in onshore coastal topography that have occurred in the past 250 years do affect the inundation. In such a situation, the numerical model, if it is sufficiently credible, offers a good means to estimate tsunami hazard information in regard to distribution of the inundation depth.

5.2 BTV assessment

This study focuses on the application of a new methodology to assess building vulnerability to the threat of tsunamis in the coastal area of Casablanca-Morocco. The proposed BTV model has two main advantages: (1) the estimation of tsunami vulnerability of building classes by the introduction of building types with similar conditions in the same class, which permits the assessment of BTV for a larger area containing various building

types; and (2) the use of tsunami inundation modelling to identify the potential zones at risk of flooding, which is particularly important in areas where tsunamis are infrequent and where no field data is available to calibrate the inundation.

On the other hand, different approaches have been recently developed to estimate the damage to buildings due to the impact of tsunami waves. Some of these approaches use the current velocity and flood force design to assess the level of damage. The BTV model proposed in this study does not integrate the current velocity and flood force in its estimation of building damage expected for three main reasons: (1) both the flood velocity and the hydrodynamic tsunami load depend on the flow depth (Dames and Moore 1980; Okada et al. 2005), which has been considered in this study to be a principal criterion in the assessment of the BTV; (2) the tsunami flood can create on the onshore buildings a large variety of forces, including hydrostatic, buoyant, hydrodynamic, surge and debris impact forces, as well as wave-breaking loads. Assessing the impact of these forces on the building is difficult due to the design of those loads and the estimation of the impact duration (Yeh 2007); and (3) the estimation of the building damage based on the tsunami forces design requires precise information concerning the mechanical behaviour laws of the building construction materials, as well as the exact geometry and building form. This kind of data is difficult to collect, especially for areas that contain a variety of building types.

Results presented within GIS in the form of a vulnerability map show a clear picture of the most vulnerable parts of Casablanca harbour and the surrounding area. This map may enable local authorities and emergency planners to construct an evacuation plan for the study area. It can also be useful for the localization of priority zones where tsunami mitigation measures must be concentrated. The very high BTV category is concentrated in the western coastal part of the area studied due to the presence of poorly constructed buildings, as well as an absence of breakwater barriers. These building types are vulnerable to total collapse in the case of a 1755-like tsunami event. Hence, this zone should benefit, whenever possible, from structure-retrofitting or rebuilding programs. The well-constructed buildings have BTVs raging from low to medium, depending on their locations. The expected damage to structures in this category may be limited to the first floor. For buildings in this class and located within a zone of high flood risk, it is recommended that any fragile material, such as glass, be avoided in first floor construction. Further, there should be a plan for vertical evacuation.

6 Conclusions

We simulated the coastal inundation for tectonic-generated tsunami sources offshore from South West Iberia. The parameters of the tsunami sources used in this study are those that have been published by other authors. The computed run-up heights range from 1 to 15 m, and the inundation areas range in distance from 0 to 1.5 km inland. The worst case scenario has been used to produce a vulnerability map. The BTV model incorporates multiple factors that contribute to tsunami vulnerability that we can divide into two main categories: a factor inherent to building condition and two parameters related to the external or environmental conditions (inundation zone and sea defence).

Most buildings, in the study area, are note configured and maintained in ways that effectively reduce the risk of exposure to the threat of tsunami. The very high tsunami vulnerability of some zones in Casablanca requires urgent tsunami mitigation planning. Also, buildings of ancient Medina, which present the historical and cultural patrimony of

Casablanca, should benefit from building restoration programs, in view of the fact that about 50% of this zone belongs to a high BTV category.

In summary, the results presented here suffer from limitations due to the models used to describe the rupture, propagation and run-up, and also from the data available concerning bathymetry, topography and buildings. Despite these limitations, the results correspond to first-hand quantification appropriate to tsunami impact and have important implications for decision makers and land use planning.

Acknowledgments This study was funded by project NEAREST—Integrated observations from NEAR shore sources of Tsunamis: towards an early warning system, contract 037110 UE, 6FP. The authors thank Dr. Eric Font for internal review of this manuscript and Professor Abdallah El Hammoumi for comments on building survey. Finally, we also thank the two anonymous reviewers for their valuable comments.

References

Abe K (1979) Size of great earthquakes of 1837–1974 inferred from tsunami data. J Geophys Res 84:1561–1568

Baptista MA, Heitor S, Miranda JM, Miranda P, Mendes Victor L (1998a) The 1755 Lisbon earthquake; evaluation of the tsunami parameters. J Geodyn 25:143–157

Baptista MA, Miranda PMA, Miranda JM, Mendes Victor L (1998b) Constrains on the source of the 1755 Lisbon tsunami inferred from numerical modelling of historical data on the source of the 1755 Lisbon tsunami. J Geodyn 25:159–174

Baptista MA, Miranda JM, Chiericci F, Zitellini N (2003) New study of the 1755 earthquake source based on multi-channel seismic survey data and tsunami modelling. Nat Hazards Earth Syst Sci 3:333–340

Boen T, EERI M (2006) Observed reconstruction of houses in Aceh seven months after the great Sumatra earthquake and Indian Ocean tsunami of December 2004. Earthq Spectra 22(S3):S803–S818

Borges JF, Fitas AJS, Bezzeghoud M, Teves-Costa P (2001) Seismotectonics of Portugal and its adjacent Atlantic area. Tectonophysics 331:373–387

Buforn E, Udías A, Mézcua J (1988) Seismicity and focal mechanisms in south Spain. Bull Seism Soc Am 78:2008–2224

Buforn E, Bezzegoud M, Udias A, Pro C (2004) Seismic sources on the Iberia-African plate boundary and their tectonic implications. Pure Appl Geophys 161:623–626

Dames, Moore (1980) Design and construction standards for residential construction in tsunami-prone areas in Hawaii. Prepared for the Federal Emergency Management Agency by Dames & Moore, Washington D.C

Debrach J (1946) Raz de marée d'origine sismique enregistré sur le littoral atlantique du Maroc (in french), Service de Physique du Globe et de l'institut scientifique Chérifien, Annales, Maroc

DeMets C, Gordon R, Argus D, Stein S (1994) Effect of recent revisions to the geomagnetic reversal time scale on estimates of current plate motions. Geophys Res Lett 21:2191–2194

Dominey-Howes D, Papathoma M (2007) Validating a tsunami assessment model (the PTVA Model) using field data from the 2004 Indian Ocean tsunami. Nat Hazards 40:113–136

El Alami SO, Tinti S (1991) A preliminary evaluation of the tsunami hazards in the Moroccan coasts. Sci Tsunami Hazards 9:31–38

El-Mrabet T (1991) Historical seismicity in Morocco (in Arabic). Thesis 3rd cycle, Letters Faculty, University of Rabat, Morocco

Fernandes RMS, Ambrosius BAC, Noomen R, Bastos L, Wortel MJR, Spakman W, Rovers G (2003) The relative motion between Africa and Eurasia as derived from ITRF2000 and GPS data. Geophys Res Lett 30(16):1828. doi:10.1029/2003GL017089

Fernandes RMS, Miranda JM, Meijninger BML, Bos MS, Noomen R, Bastos L, Ambrosius BAC, Riva REM (2007) Surface velocity field of the Ibero-Maghrebian segment of the Eurasia-Nubia plate boundary. Geophys J Int 169(1):315–324 (APR)

Fukao Y (1973) Thrust faulting at a lithosphere plate boundary. The Portugal earthquake of 1969. Earth Planet Sci Lett 18:205–216

Gjevik B, Pederson G, Dybesland E, Miranda PM, Baptista MA, Heinrich P, Massinon B (1997) Modelling tsunamis from earthquake sources near Gorringe Bank Southwest of Portugal. J Geophys Res 102:27931–27949

Gutscher M-A (2004) What caused the great Lisbon earthquake? Science 305:1247–1248

Gutscher M-A, Malod J, Rehault J-P, Contruci I, Klingelhoefer F, Mendes-Victor L, Spakman W (2002) Evidence for active subduction beneath Gibraltar. Geology 30(12):1071–1074
Gutscher M-A, Baptista MA, Miranda JM (2006) The Gibraltar Arc seismogenic zone (part 2): constraints on a shallow east dipping fault plane source for the 1755 Lisbon earthquake provided by tsunami modelling and seismic intensity. Tectonophysics 426:153–166
Jiménez-Munt I, Fernàndez M, Torne M, Bird P (2001) The transition from linear to diffuse plate boundary in the Azores-Gibraltar region: results from a thin sheet model. Earth Planet Sci Lett 192:175–189
Johnston A (1996) Seismic moment assessment of earthquakes in stable continental regions—III. New Madrid, 1811—1812, Charleston 1886 and Lisbon 1755. Geophys J Int 126:314–344
Lander JF, Whiteside LS, Lockridge PA (2002) Brief history of Tsunamis in the Caribbean Sea. Sci Tsunami Hazards 20(2):57–94
Lander JF, Whiteside LS, Lockridge PA (2003) Two decades of global tsunamis 1982–2002. Sci Tsunami Hazards 21(1):3–88
Levret A (1991) The effects of the November 1, 1755 "Lisbon" earthquake in Morocco. Tectonophysics 193:83–94
Liu PL-F, Cho Y-S, woo S-B, Seo SN (1994) Numerical simulations of the 1960 Chilean tsunami propagation and inundation at Hilo, Hawaii. In: El-Sabh MI (ed) Recent developments in tsunami research. Kluwer, Dordrecht, pp 99–115
Liu PL-F, Cho Y-S, Brrigs MJ, Kanoglu U, Synolakis CE (1995) Runup of solitary waves on a circular island. J Fluid Mech 302:259–285
Liu PL-F, Woo S-B, Cho Y-S (1998) Computer programs for tsunami propagation and inundation. Cornell University, New York
Maheshwari BK, Eery E, Sharma ML, Narayan JP (2006) Geotechnical and structural damage in Tamil Nadu, India, from the December 2004 Indian Ocean tsunami. Earthq Spectra 22(S3):S321–S354
Mansinha L, Smylie DE (1971) The displacement field of inclined faults. Bull Seism Soc Am 61:1433–1440
Martinez-Solares JM, Lopez A, Mezcua J (1979) Isoseismal map of the 1755 Lisbon earthquake obtained from Spanish data. Tectonophysics 53:301–313
Miranda JM, Mendes Victor LA, Simões JZ, Luis JF, Matias L, Shimamura H, Shiobara H, Nemoto H, Mochizuki H, Hirn A, Lépine JC (1998) Tectonic setting of the Azores Plateau deduced from a OBS survey. Mar Geophys Res 20(3):171–182
Morel JL, Meghraoui M (1996) Goringe-Alboran-Tell tectonic zone: a transpression system along the Africa-Eurasia plate boundary. Geology 24:755–758
Murty CVR, EERI M, Rai DC, Jain SK, Kaishik G, Dach SR (2006) Performance of structures in the Adaman and Nicobar islands (India) during the December 2004 great Sumatra earthquake and Indian Ocean tsunami. Earthq Spectra 22(S3):S475–S493
Okada Y (1985) Surface deformation due to shear and tensile faults in a half-space. Bull Seism Soc Am 75:1135–1154
Okada T, Sugano T, Ishikawa T, Ohgi T, Takai S, Hamabe C (2005) Structural design method of buildings for tsunami resistance (proposed). Building Technology Research Institute, Building Centre for Japan, p 15
Okal EA, Synolakis CE (2004) Source discriminants for near-field tsunamis. Geophys J Int 158:899–912
Papathoma M, Dominey-Howes D (2003) Tsunami vulnerability assessment and its implications for coastal hazard analysis and disaster management planning, Gulf of Corinth, Greece. Nat Hazard Earth Syst Sci 3(6):733–744
Papathoma M, Dominey-Howes D, Zong Y, Smith D (2003) Assessing tsunami vulnerability, an example from Heraklion, Crete. Nat Hazard Earth Syst Sci 3:377–389
Reese S, Cousins WJ, Power WL, Palmer NG, Tejakusuma IG, Nugarahadi S (2007) Tsunami vulnerability of buildings and people in South Java-field observation after the July 2006 Java tsunami. Nat Hazard Earth Syst Sci 7:573–589
Roest WR, Srivastava SP (1991) Kinematics of the plate boundaries between Eurasia, Iberia, and Africa in the North Atlantic from the Late Cretaceous to the present. Geology 19:613–616
RPS2000 (2000) Reglement de construction paraseismique au Maroc (in french). http://www.structureparasismic.com/PdvRps2000.htm
Ruangrassamee A, Yanagisawa H, Foytong P, Lukkunaprasit P, Koshimura S, Imamura F (2006) Investigation of tsunami-induced damage and fragility of buildings in Thailand after the December 2004 Indian Ocean tsunami. Earthq Spectra 22(S3):S377–S401
Saatcioglu M, EERI M, Ghobarah A, Nistor I (2006) Performance of structural in Thailand during the December 2004 great Sumatra earthquake and Indian Ocean tsunami. Earthq Spectra 22(S3):S355–S375
Sartori R, Torelli L, Zitellini N, Peis D, Lodolo E (1994) Eastern segment of the Azores-Gibraltar line (central-eastern Atlantic): an oceanic plate boundary with diffuse compressional deformation. Geology 22:555–558

Sella GF, Dixon TH, Mao A (2002) REVEL: a model for recent plate velocities from space geodesy. J Geophys Res 107(B4):2081. doi:10.1029/2000JB000033

Synolakis CE, Bernard EN, Titov VV, Kânoğlu U, González FI (2007) Standards, criteria, and procedures for NOAA evaluation of tsunami numerical models. NOAA Tech Memo OAR PMEL-135, NTIS: PB2007–109601, NOAA/Pacific Marine Environmental Laboratory, Seattle, p 55

Thiebot E, Gutscher M-A (2006) The Gibraltar Arc seismogenic zone (part 1): constraints on a shallow east dipping fault plane source for the 1755 Lisbon earthquake provided by seismic data, gravity and thermal modeling. Tectonophysics 426:135–152

Tortella D, Torne M, Pérez-Estaún A (1997) Geodynamic evolution of the eastern segment of the Azores-Gibraltar zone: the Gorringe Bank and the Gulf of Cadiz region. Mar Geophys Res 19:211–230

Wang X, Liu PL-F (2005) A numerical investigation of Boumerdes-Zemmouri (Algeria) earthquake and tsunami. Comput Model Eng Sci 10(2):171–184

Wang X, Liu PL-F (2007a) Numerical simulations of the 2004 Indian Ocean tsunamis—coastal effects. J Earthq Tsunami 1(3):273–297

Wang X, Liu PL-F (2007b) COMCOT user manual-version 1.6. School of Civil and Environmental Engineering, Cornell University Ithaca, NY 14853, USA. http://ceeserver.cee.cornell.edu/pll-group/doc/comcot_user_manual_v1_6.pdf

Yeh H (2007) Design tsunami forces for onshore structures. J Disaster Res 2:531–536

Zitellini N, Chierici F, Sartori R, Torelli L (1999) The tectonic source of the 1755 Lisbon earthquake. Ann Geofis 42(1):49–55

Zitellini N, Mendes L, Cordoba D, Dañobeitia JJ, Nicolich R, Pellis G, Ribeiro A, Sartori R, Torelli L (2001) Source of the 1755 Lisbon earthquake and tsunami investigated. Eos Trans AGU 82(26): 285–291